Supplementary Material for

One-pot mechanochemical ball milling synthesis of the MnO_x nanostructures as efficient catalysts for CO_2 hydrogenation reaction

Altantuya Ochirkhuyag[a], András Sápi[ab*], Gábor Kozma[a], Ákos Szamosvölgyi[a], Ákos Kukovecz[ac], Zoltán Kónya[ac]

[a] *University of Szeged, Interdisciplinary Excellence Centre, Department of Applied and Environmental Chemistry, H-6720, Rerrich Béla tér 1, Szeged, Hungary*

[b] *Institute of Environmental and Technological Sciences, University of Szeged, H-6720, Szeged, Hungary*

[b] *MTA-SZTE Reaction Kinetics and Surface Chemistry Research Group, University of Szeged, H-6720 Szeged, Rerrich Béla tér 1, Szeged, Hungary*

**corresponding authors: sapia@chem.u-szeged.hu*

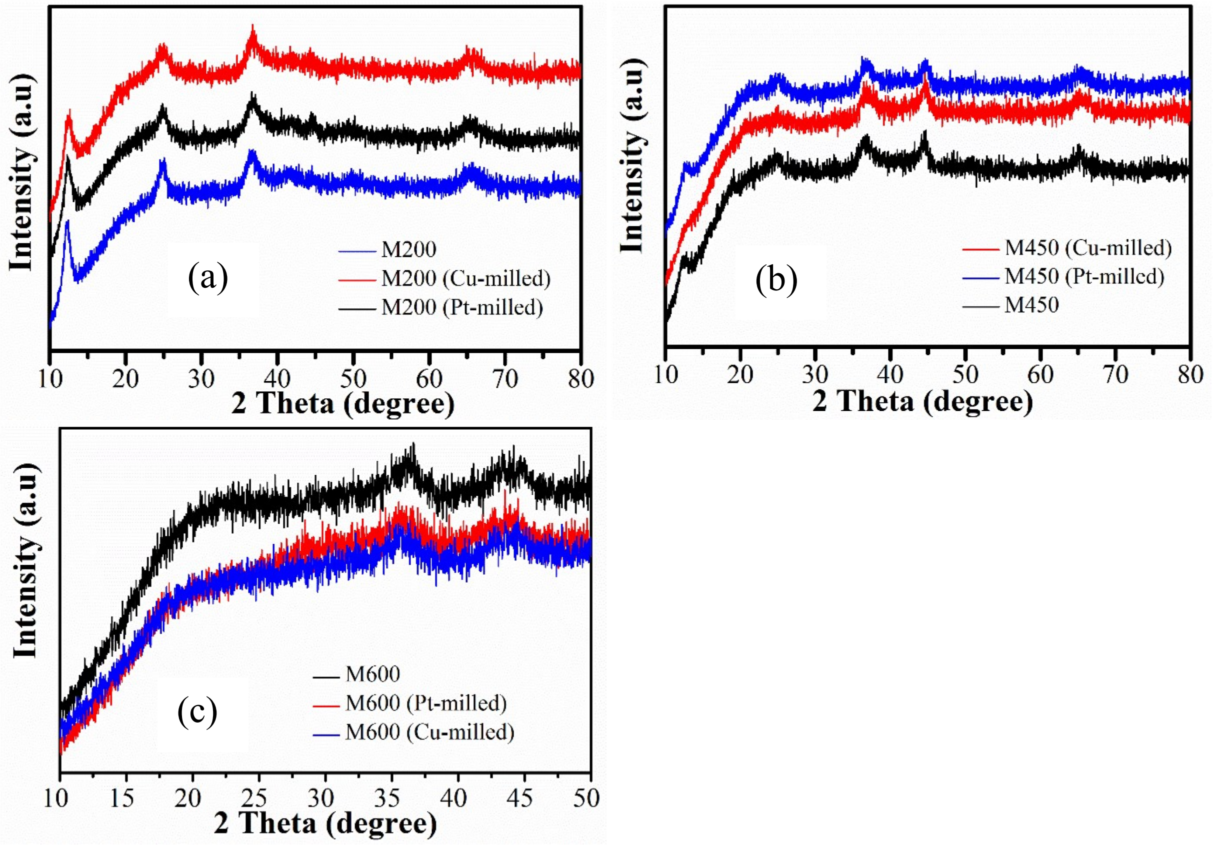

Figure S1. X-ray diffraction patterns M200 sample (pure, metal (Pt and Cu) doped) (a), M450 (pure, metal Pt/Cu doped) (b) and M600 (pure, metal Pt/Cu doped) samples (c).

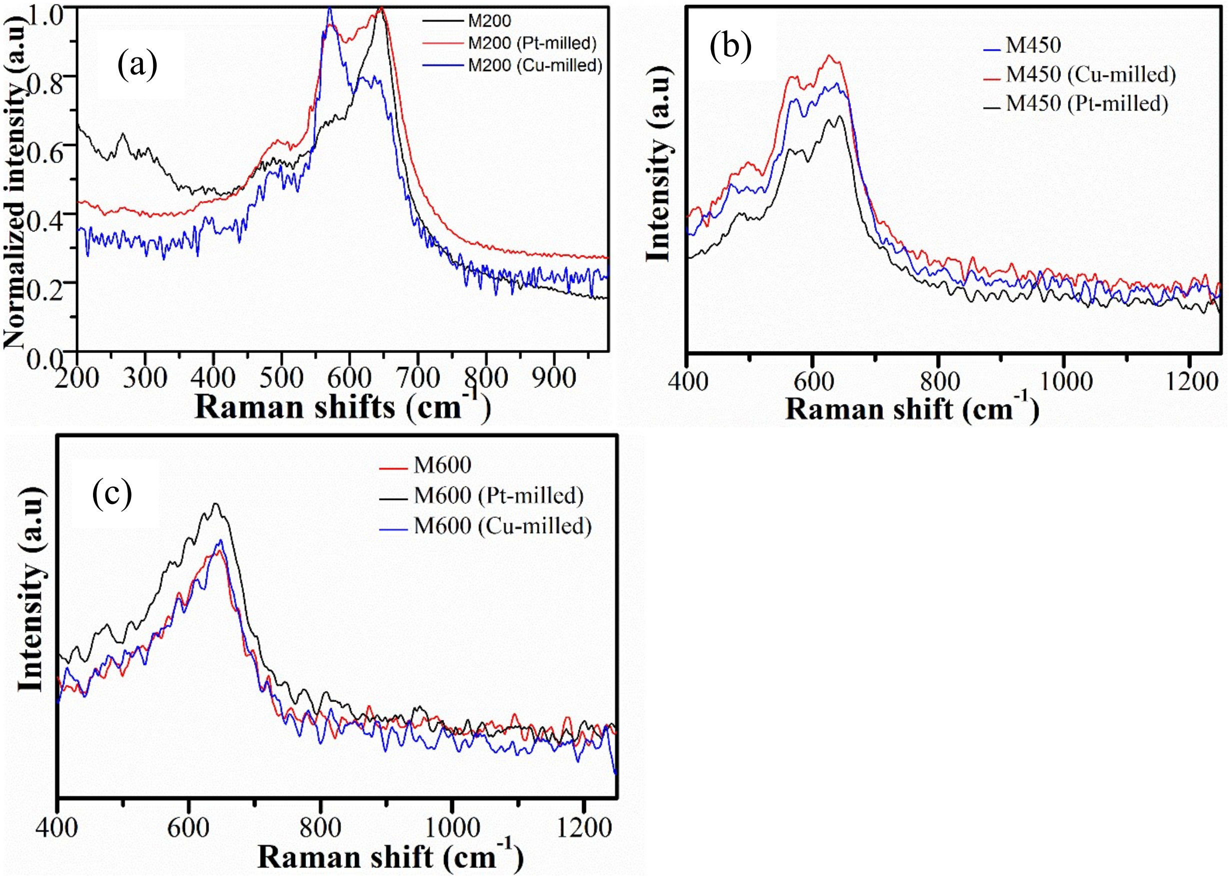

Figure S2. Normalized Raman shifts of the M200 sample (pure, metal (Pt and Cu) doped) (a), M450 (pure, metal Pt/Cu doped) (b) and M600 (pure, metal Pt/Cu doped) samples (c).

Table S1. Composition of the manganese oxide catalysts evaluated from SEM-EDS data

Sample	Composition **(at. %**)						Composition **wt.%**					
	Mn	K	O	Na	**Pt**	**Cu**	Mn	K	O	Na	**Pt**	**Cu**
M200	27.77	0.90	64.81	6.51	-		55.53	1.28	37.74	5.45	-	-
M450	21.90	0.29	73.32	4.49	-		48.31	0.46	47.09	47.09	-	-
M600	16.80	0.11	80.46	2.64	-		40.56	0.18	56.59	2.67	-	-
M600 (Pt-milled)	19.11	0.51	71.28	8.70	**0.39**		42.21	0.80	45.86	8.04	**3.09**	-
M450 (Cu-milled)							42.60	0.59	49.45	5.81	-	**1.55**

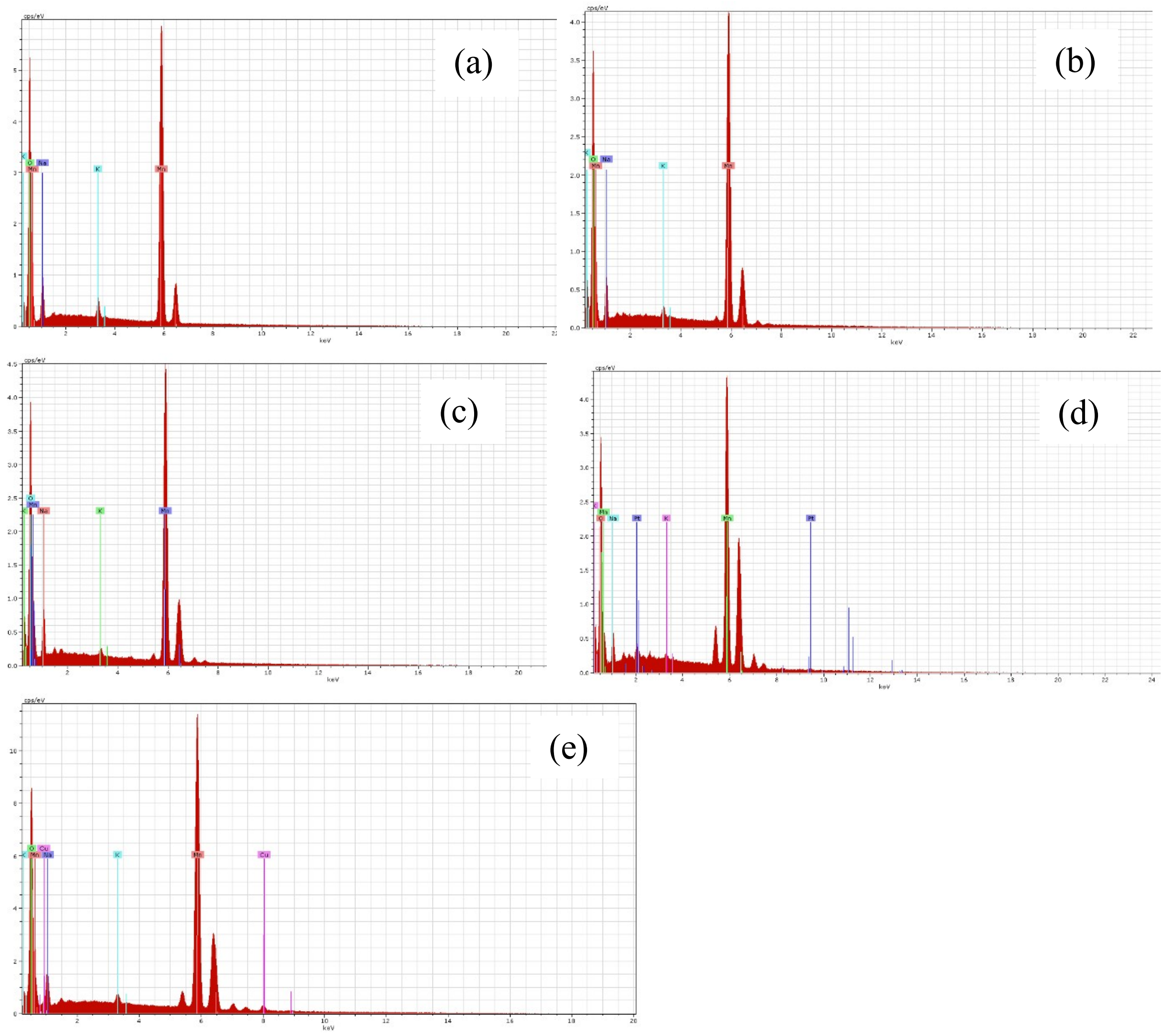

Figure S3. EDX spectra of the milled pure sample (a) M200 pure, (b) M450 pure, (c) M600 pure, (d) M600 doped (Pt- milled) and (e) M450 doped (Cu-milled).

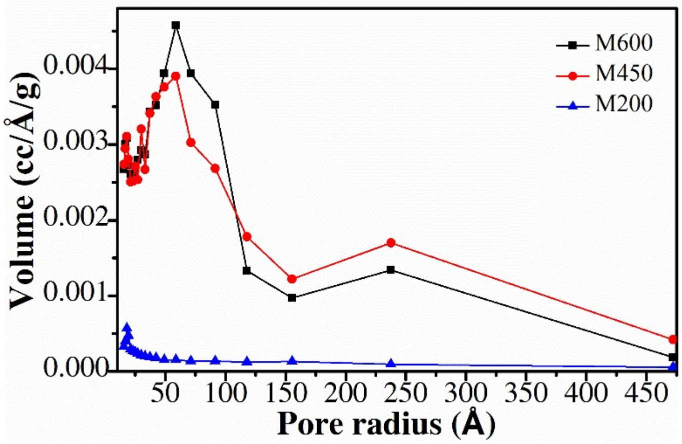

Figure S4. The pore radius of the pure samples calculated from BET evaluation of N_2 adsorption-desorption isotherms

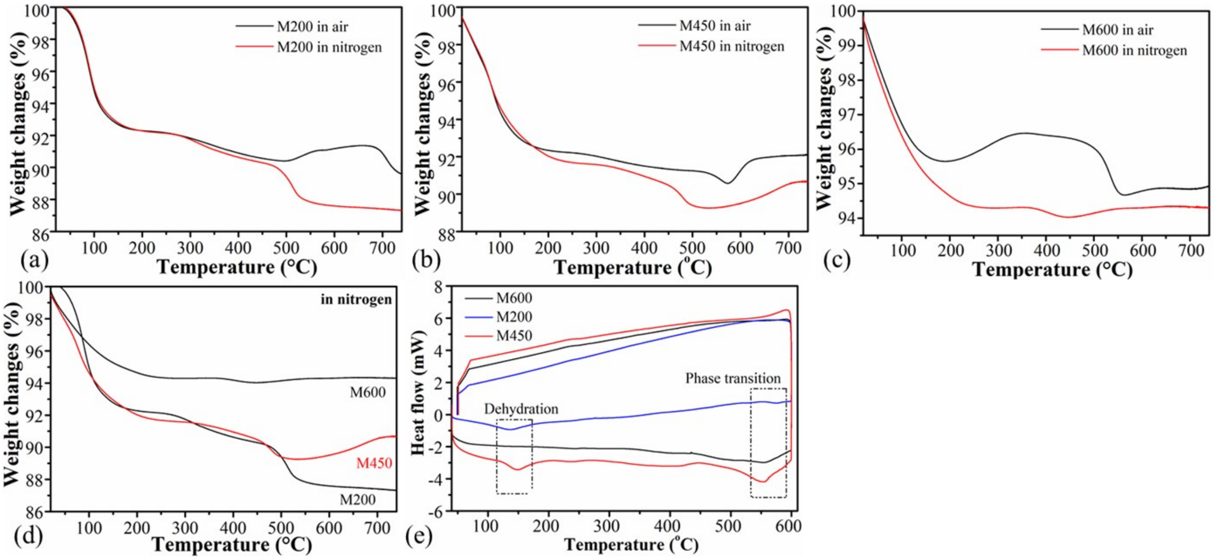

Figure S5. Thermogravimetric analysis of the samples in air and nitrogen (a-c), and all three samples in nitrogen (d) and differential scanning calorimetry results of the milled samples in nitrogen (e).

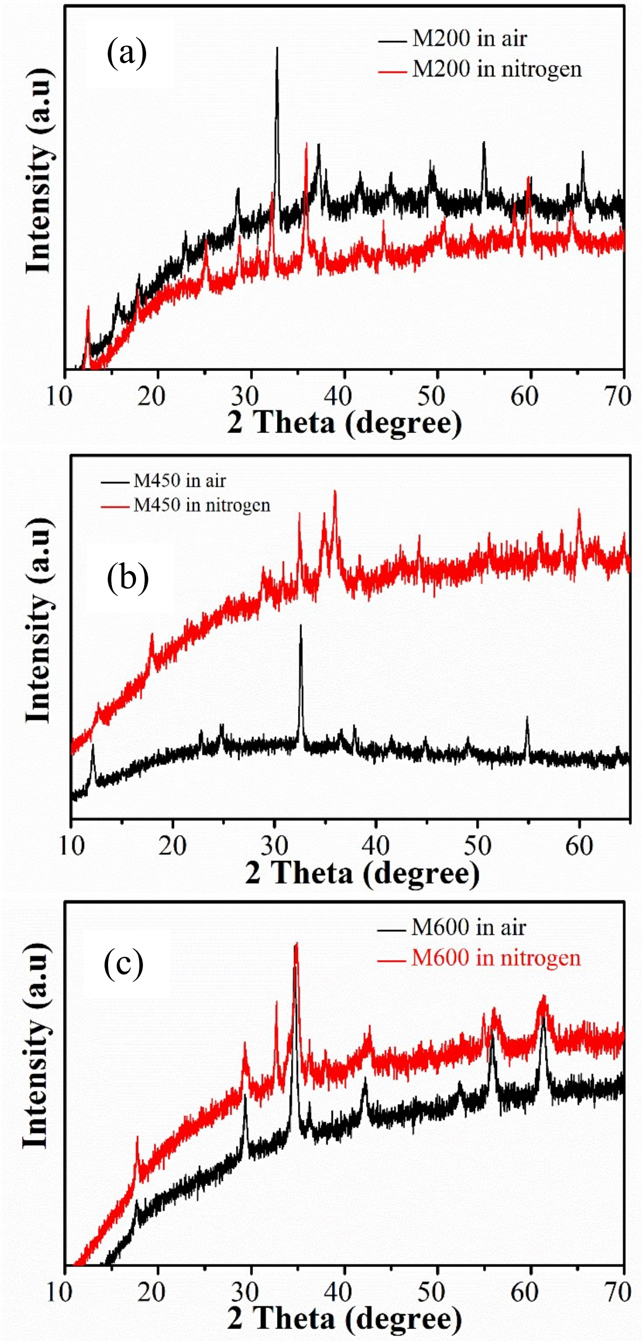

Figure S6. X-ray diffraction patterns of the samples after TGA analysis: a) M200, c) M450, and b) M600.

Pretreatment:

X-ray diffraction patterns of the samples disclosed in pretreated samples (before CO_2 hydrogenation test) in **Fig S7a** and after hydrogenation in **Fig S7b**. Pretreatment used H_2 gas as a reducing agent, and the manganese oxidation state partially reduced to Mn^{+3} and Mn^{+2}. Nevertheless, Mn^{+4} is still in the structure after pretreatment mainly for the sample M200 and M450. After the pretreatment, tunnel structure generated caused by the increases of distinction of Mn^{4+} and Mn^{3+} ion ratio in the crystal structure and decreases of the interlayer water and cations. In **Fig 7 b**, diffraction patterns compromise that manganese (II) oxide (MnO) is the remained product after the CO_2 hydrogenation test.

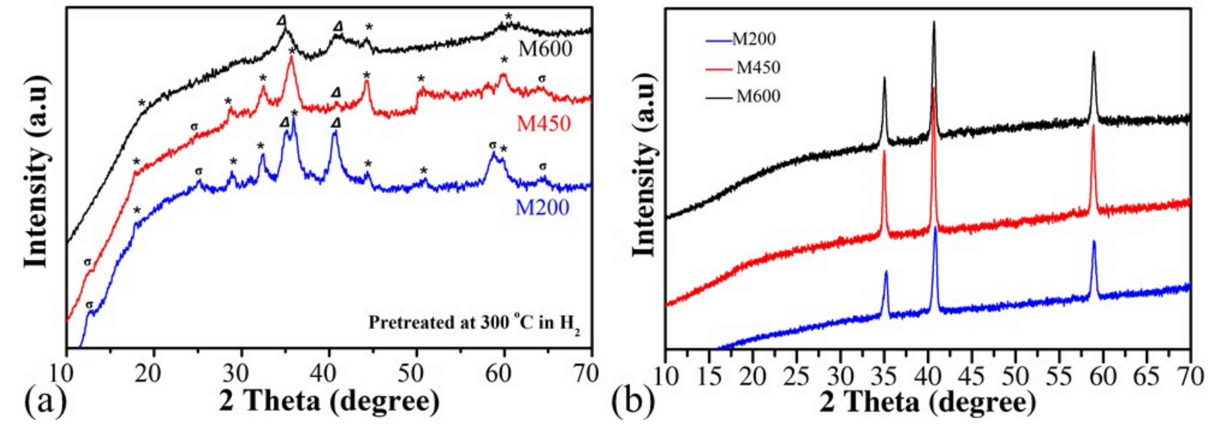

Figure S7. X-ray diffraction patterns of the samples {{* *birnessite type σ-MnO_2,* ■ *Mn_3O_4 phase*, **Δ**-MnO phase} pretreated (a) and after CO_2 hydrogenation test (b).

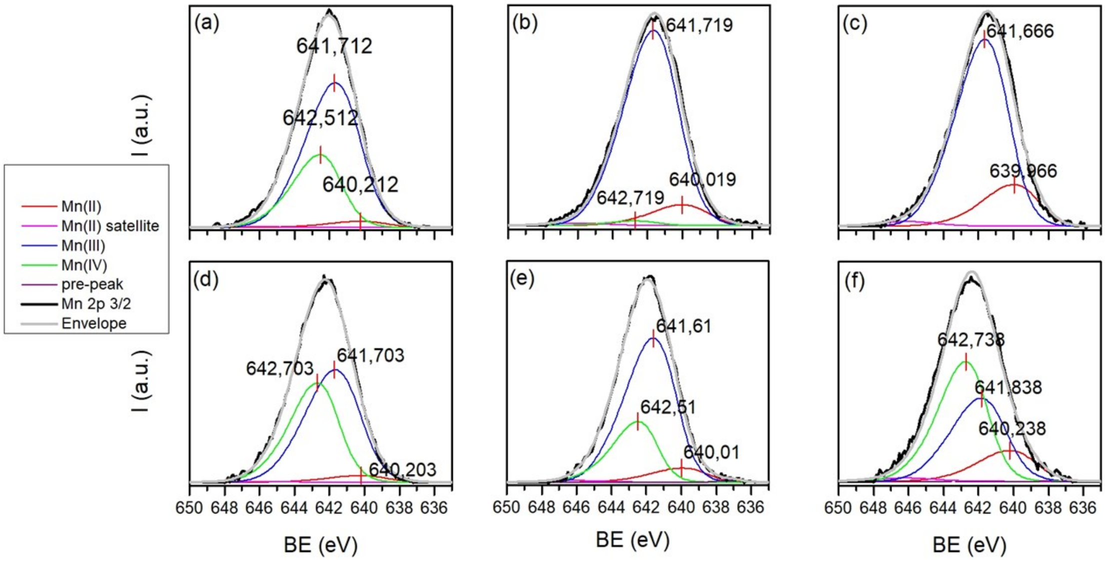

Figure S8. The collected Mn 2p 3/2 spectra of the different MnOx samples, (a) M200 after pretreatment, (b) M600 after pretreatment, (c) Pt-milled M600 after pretreatment and (d) M600 after the reaction (e) Pt-milled M600 after pretreatment, (f) Pt-milled M600 after the reaction.

Table S2. Atomic ratios of Mn oxidation states in the analysed samples.

	%pre-peak	%Mn(II)	%Mn(II) satellite	%Mn(III)	%Mn(IV)	RSTD
M200 pretreated	0	2.95	0.34	66.6	30.45	1.17
M600 pretreated	0	9.88	1.11	88.25	1.87	1.48
Pt-milled M600 pretreatment	0	19.04	2.12	80.96	0	1.61
M200 after reaction	0	3.3	0.37	53.68	43.02	1.07
M600 after reaction	0.43	6.95	0.78	67.59	25.45	0.99
Pt-milled M600 after reaction	0.02	14.38	1.61	37.1	48.51	1.59